

Dynamic simulation model of a parabolic trough collector system with concrete thermal energy storage for process steam generation

Cite as: AIP Conference Proceedings **2126**, 150007 (2019); <https://doi.org/10.1063/1.5117663>
Published Online: 26 July 2019

Johannes Christoph Sattler, Spiros Alexopoulos, Ricardo Alexander Chico Caminos, John Mitchell, Víctor Ruiz, Soteris Kalogirou, Panayiotis Ktistis, Cristiano Teixeira Boura, and Ulf Herrmann



View Online



Export Citation

ARTICLES YOU MAY BE INTERESTED IN

[Analysis of volumetric solar radiation absorbers made of wire meshes](#)

AIP Conference Proceedings **2126**, 030009 (2019); <https://doi.org/10.1063/1.5117521>

[“MOSAIC”, A new CSP plant concept for the highest concentration ratios at the lowest cost](#)

AIP Conference Proceedings **2126**, 060008 (2019); <https://doi.org/10.1063/1.5117594>

[Realization of a test rig for small solar collectors and preliminary test](#)

AIP Conference Proceedings **2126**, 120016 (2019); <https://doi.org/10.1063/1.5117634>

Lock-in Amplifiers
up to 600 MHz



Dynamic Simulation Model of a Parabolic Trough Collector System with Concrete Thermal Energy Storage for Process Steam Generation

Johannes Christoph Sattler^{1, a)}, Spiros Alexopoulos², Ricardo Alexander Chico Caminos², John Mitchell³, Victor Ruiz⁴, Soteris Kalogirou⁵, Panayiotis Ktistis⁵, Cristiano Teixeira Boura², Ulf Herrmann²

¹M.Sc., Project Engineer, Solar-Institut Jülich of the Aachen University of Applied Sciences (SIJ), Heinrich-Mussmann-Str. 5, 52428 Jülich, Germany

²Solar-Institut Jülich of the Aachen University of Applied Sciences (SIJ), Heinrich-Mussmann-Str. 5, 52428 Jülich, Germany

³Protarget AG, Zeissstrasse 5, 50859 Cologne, Germany

⁴CADE Soluciones de Ingeniería, S.L., Parque Científico y Tecnológico, Paseo de la Innovación, 3, 02006 Albacete, Spain

⁵Cyprus University of Technology, 30 Arch. Kyprianos Str., 3036 Limassol, Cyprus

^{a)}Corresponding author: sattler@sj.fh-aachen.de

Abstract. Parabolic trough collector (PTC) systems are commercially available concentrating solar power plants widely known for their application to generate electrical power. To further reduce the dependency on fossil fuels, such systems can also be deployed for producing process heat for industrial purposes. In combination with a thermal energy storage system, this technology has the ability to reliably supply on-demand process heat. This paper gives details on a fully automated PTC system with concrete thermal energy storage (C-TES) and kettle-type boiler that supplies saturated steam for a beverage factory in Limassol, Cyprus. In the focus is the validation of a dynamic simulation model in Modelica[®] that physically describes the entire PTC system. The simulation model uses various plant data as inputs including mirror reflectivity and weather data from on-site measurements. The validation was carried out in three steps. First, the PTC was validated as a stand-alone component. A time-dependent inlet oil temperature vector was given as input and the outlet oil temperature was computed. The root mean square (rms) error between the measured to simulated outlet oil temperature values results in 3.86% (equivalent to about 1.9K). The second part of the validation then considered a complete PTC oil cycle in PTC-and-boiler operation mode (without C-TES). In the simulation, both the PTC inlet and outlet oil temperatures were computed. The result is a deviation < 4.25% (rms) between measured to simulated values. Finally, in the third step, the C-TES model was validated as a stand-alone component. The deviation between measurement and simulated values is < 5% compared to the design point.

INTRODUCTION

The application of parabolic trough collector (PTC) systems for producing process steam for industrial applications is gaining international importance. With 33 PTC systems installed worldwide, the food and beverage industry clearly dominates as target industry. Further 15 plants exist for 10 other industrial applications. [1]

In Limassol, Cyprus, a fully automated PTC system with concrete thermal energy storage (C-TES) was installed as part of an international research project. The system is designed to produce up to 5% of the process steam demand of the local beverage factory KEAN Soft Drinks Ltd. This leads to a reduction in the fossil fuel consumed by the factory's gas-fired boiler and hence to lower fuel costs and CO₂ emissions. The PTC system is manufactured by Protarget AG, Germany, and the C-TES by CADE Soluciones de Ingeniería, S.L., Spain.

In the focus of this paper is a dynamic simulation model developed by the Solar-Institut Jülich (SIJ) that simulates the entire PTC system with C-TES for steam generation. The simulation model is used for several purposes including (i) improving the plant's controller, (ii) to simulate adjusted operating strategies prior implementation in the process control system of the real plant, and (iii) to make accurate energy yield and plant efficiency predictions for scaled-up systems. The simulation model was developed using Modelica[®] language. The local project partner Cyprus University of Technology provides SIJ with weekly mirror reflectivity measurement and weather data, which serve as input for the simulation model.

DESCRIPTION OF PTC SYSTEM WITH C-TES FOR STEAM GENERATION

A schematic of the installed plant is shown in Fig. 1 (a) below. The key components are a two-row PTC field with a total length of 96 m, a two-module C-TES (TES 1 and TES 2), a kettle-type boiler and a thermal oil pump. The oil temperature measurement points are marked as T1 and T2. The collector rows are not aligned in north-south direction due to land restrictions. Each of the C-TES modules consists of two insulated sub-modules of each 5 m length placed next to each other in a shipping container. Fig. 1 (b) shows the insulated sub-modules. Each sub-module is designed with 20 tubes arranged in a 5-by-4 matrix. The C-TES has a capacity of 600 kWh allowing on-demand and continuous supply of steam. The PTC has a mid-sized aperture of 3 m and is equipped with a novel heat collecting element (HCE) as shown in Fig. 1 (c). The HCEs diameter is specially adapted to the collector's aperture in order to maximise the collector's efficiency. The thermal oil deployed in the plant is HELISOL XA, which can be heated to 425 °C. Fig. 1 (d) shows the PTC in solar operation during the commissioning phase together with a weather station.

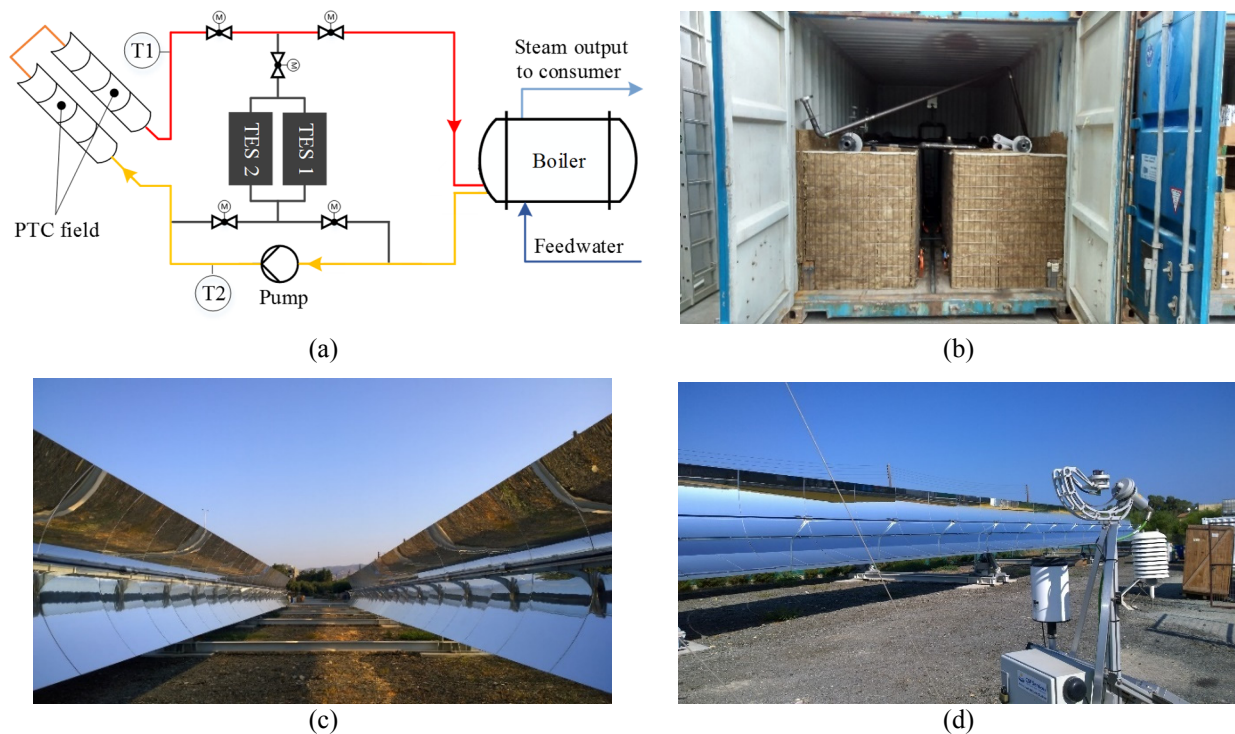


FIGURE 1. (a) Schematic representation of the PTC system with C-TES (modules installed in parallel). (b) Photo of a single C-TES module consisting of two sub-modules placed in a shipping container during the installation phase (Photo provided by and © CADE). (c) Two-row PTC system (Photo provided by and © Protarget). (d) Photo showing the PTC system in solar operation and the weather station during the commissioning phase (Photo provided by and © Protarget).

The temperature control is realised solely via a thermal oil temperature measurement coupled with tailored algorithms for mass flow control. Although usually used in conventional PTC plants the direct normal irradiance (DNI) is not a controller input. The plant operation is controlled using a controller with integrated operating strategies for handling varying steam demand profiles and operating states during all types of weather conditions. Even though

the system is principally capable of producing process heat to enable 24/7 operation, the KEAN factory requires steam for only up to 16 hours. The solar system is currently going through the commissioning phase.

DYNAMIC SIMULATION MODEL OF THE PTC SYSTEM WITH C-TES

The overall model of the PTC system with C-TES, shown in Fig. 2 (a), consists of the parabolic trough collector array, the boiler, the C-TES, a superordinated plant controller, several auxiliary components such as valves V1 to V5 as well as time-dependent inputs like weather data. Each of these components contains nested layers with classes that realistically depict the physical component design and energy transfer processes.

The PTC model is composed of three layers. The third layer, shown in Fig. 2 (b), is a thermal resistance model of the HCE and consists of in-house classes.

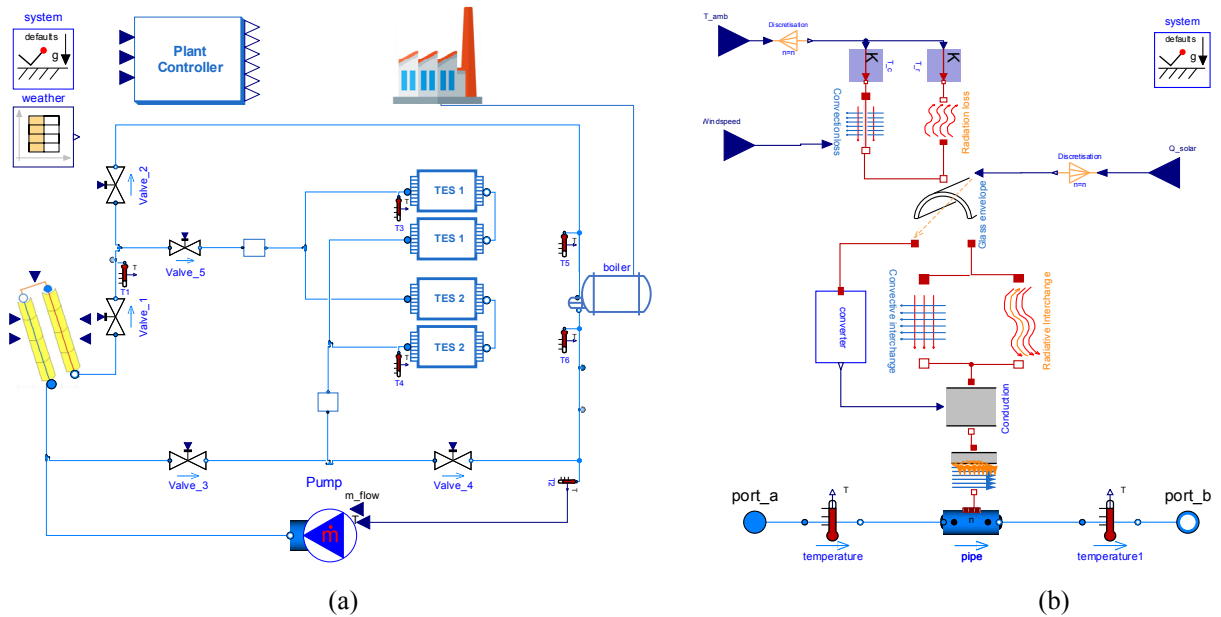


FIGURE 2. (a) Top layer class of the overall PTC system. In the interest of clarity, the depiction is simplified and shown without insulated piping. (b) HCE model with thermal resistance classes. (Both images © SIJ)

The PTC model is highly detailed in order to achieve the highest possible accuracy while still maintaining an acceptable simulation speed. Figure 3 shows a cross-sectional view of the HCE with all energy flows entering and leaving the HCEs boundaries. A HCE is fundamentally composed of a steel absorber tube (AT) with selective coating that carries a heat transfer fluid inside, a glass envelope (GE) that maintains a vacuum in the annulus, a getter, two glass-to-metal seals as well as two bellows. To describe the HCE mathematically it is necessary to define two boundaries and three transient energy balances (here the unit of the variables' is in W/m^2). Boundary 1 is split into two boundaries, namely 1,i and 1,o (where "i" stands for inside and "o" stands for outside). With the first energy balance (Eq. 1), the glass envelope temperature of the HCE is computed. The rate of change of energy stored in the glass envelope's material is the expression on the left hand side of the equation. The running index i and time t are written in superscript to indicate that the simulation model is discretised and transient. The DNI passes through boundary 1,o (cf. Fig. 3) of which a portion is absorbed by the glass as $\dot{q}_{e,abs}^{i,t}$. There is also a radiation exchange between the AT and the GE, $\dot{q}_{ea,rad}^{i,t}$ entering through boundary 1,i into the glass material as well as the loss due to convection in the annulus, $\dot{q}_{ann,conv}^{i,t}$. Leaving boundary 1,o are the radiation loss from the GE to the atmosphere, $\dot{q}_{e,rad}^{i,t}$, and also the convection loss to the atmosphere due to natural or forced convection depending on the wind speed, $\dot{q}_{e,conv}^{i,t}$. The equations are based on various sources [2-7].

$$\rho_e \cdot c_e \cdot A_e \cdot \frac{\partial T_e^i}{\partial t} = \dot{q}_{e,abs}^{i,t} + \dot{q}_{ea,rad}^{i,t} + \dot{q}_{ann,conv}^{i,t} - \dot{q}_{e,rad}^{i,t} - \dot{q}_{e,conv}^{i,t} \quad (1)$$

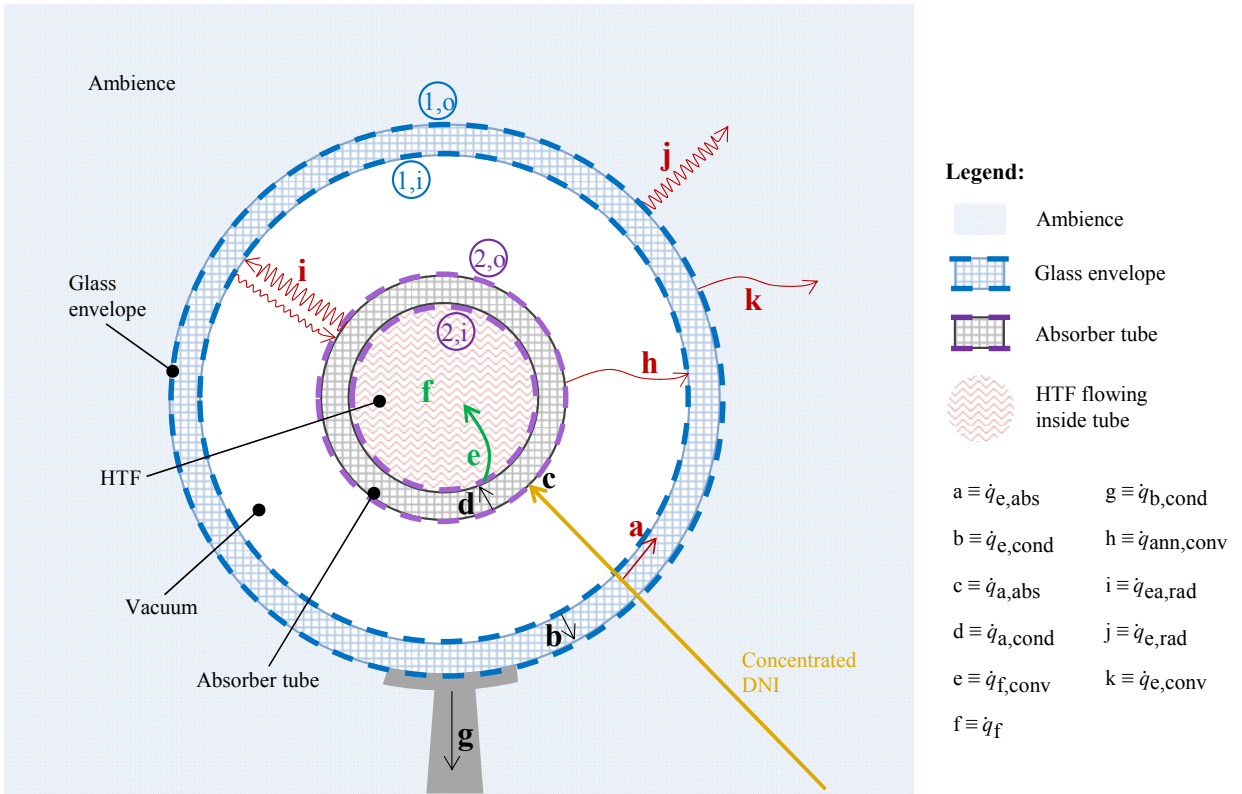


FIGURE 3. Energy balance for the heat collecting element (cross-sectional view). (© SIJ).

The second energy balance (Eq. 2) is required for determining the absorber tube temperature. The rate of change of energy stored in the absorber pipe wall is the expression on the left hand side of the equation. Entering the boundary 2,0 is the DNI of which a large proportion is absorbed as $\dot{q}_{a,abs}^{i,t}$. Leaving through boundary 2,i is the heat transferred from the absorber to the fluid, $\dot{q}_{f,conv}^{i,t}$. Leaving through boundary 2,0 towards the GE are the radiation exchange between the AT and the GE, $\dot{q}_{ea,rad}^{i,t}$, the losses due to convection in the annulus, $\dot{q}_{ann,conv}^{i,t}$, as well as the bracket loss $\dot{q}_{bracket,conv}^{i,t}$.

$$\rho_a \cdot c_a \cdot A_a \cdot \frac{\partial T_a^i}{\partial t} = \dot{q}_{a,abs}^{i,t} - \dot{q}_{f,conv}^{i,t} - \dot{q}_{ea,rad}^{i,t} - \dot{q}_{ann,conv}^{i,t} - \dot{q}_{bracket,conv}^{i,t} \quad (2)$$

The third energy balance (Eq. 3) calculates the temperature of the thermal oil flowing through the absorber tube. The rate of change of energy removed by the fluid is the expression on the left hand side of the equation. Entering the boundary 3 is the heat transferred from the absorber to the fluid, $\dot{q}_{f,conv}^{i,t}$. Leaving the boundary is the energy in the fluid, $\dot{q}_f^{i,t}$.

$$\rho_f \cdot c_f \cdot A_a \cdot \frac{\partial T_{f,i}}{\partial t} = - \dot{q}_f^{i,t} + \dot{q}_{f,conv}^{i,t} \quad (3)$$

The PTC model is discretised into 8 sections of each 12 m length. Inputs for each of the sections are the weather data as well as mirror reflectivity values obtained from weekly mirror measurements using a CONDOR reflectometer from Abengoa Solar. Reflectivity measurements are taken on the edge and in the middle of the mirror every 12 m distance along each collector row. Three reflectivity values are recorded at each measurement point. For each 12 m

section an overall average value is then computed from the outer and inner reflectivity values. Reflectivity measurements are taken every 7 days as well as before and after precipitations, and in times with above average dust concentrations in the troposphere. In order to prevent the mirror reflectivity of dropping below 88%, the mirrors are washed every 7 days. A MDI automatic weather station from CSP Services installed on the factory's site records local data of the ambient temperature, humidity and pressure, precipitation, wind speed and direction, global horizontal irradiance (GHI) as well as the direct normal irradiance (DNI). The DNI is measured with a Twin Rotating Shadowband Irradiometer (RSI) in 30-second intervals with an annual uncertainty of usually <2% [8].

Generally, when installing solar process heat systems in industrial areas, available ground is often confined and the shadows cast by close-by tall buildings and trees can pose a problem. In the case for the KEAN factory two buildings and two trees are located to the west of the PTC system and are as close as 28 m to the first collector row. This leads to a shadowing of parts of the collectors in the late afternoons within the last 60 minutes before sunset. At this time the DNI is already very low and additionally collector row shadowing also occurs. To account for the losses, the time-varying shadowed mirror area caused by two factory buildings and two trees is an input for the simulation model. Fig. 4 (a) shows a photograph which includes one of the two buildings that casts a shadow on the collector rows. Unavoidably, the weather station is also affected by the shadowing leading to short daily gaps in the DNI data which must be accounted for in the simulation of the PTC system. For calculating these building shadow losses, a separate code named Building and Tree Shadow Analyser (BTSA) was written in MATLAB®. The tool computes the shadow polygons cast on the ground for the two buildings as well as the collectors, as visually shown in Fig. 4 (b), and then subtracts one from another. This is carried out for each collector segment in order to obtain the shadow percentage values. [9]



FIGURE 4. (a) PTC in the vicinity of buildings and trees (© Protarget). (b) Computed shadow area polygons for building 1 and building 2. Computed shadow area polygons of collector row 1 (12 metre segments S1 to S4) as well as collector row 2 (segments S5 to S8). The area encompassed by a thick black line is the shadow area cast onto collector 1 by building 1. The area encompassed by the thick red line represents the shadowing of collector row 1 onto collector row 2. (© SIJ)

To model the C-TES, a single tube with a square concrete section around it is defined as a single storage element, as shown in Fig. 5. This single storage element is then divided into four quadrants. In the Modelica® model, the quadrant is discretised into 11 layers (see quadrant Q1 in Fig. 5). The C-TES model is mathematically described in a similar way as the PTC model. The single storage element is defined to have three system boundaries (of which only two are shown in Fig. 5) and comprises four energy balances. The first energy balance is used to calculate the heat exchange between the thermal oil flowing through the tube, \dot{q}_f , and the tube's wall by means of forced convection, $\dot{q}_{f,conv}$ (passing through boundary 1,i). Using the second energy balance the heat conduction through the tube wall, $\dot{q}_{w,cond}$, is determined. With the third energy balance the heat stored in or removed from the concrete material, $\dot{q}_{c,cond}$, is computed (heat passes through boundary 1,o). The fourth energy balance comprises the heat exchange with the insulation material. Note that the fourth energy balance is required only for the outermost tubes-concrete elements of the storage. In addition, as the insulation is in contact with the atmosphere inside the container, the radiation and convection losses are also computed. To allow a temporal and spacial computation of the energy content along the length, the storage model is discretised into several individual blocks of equal length.

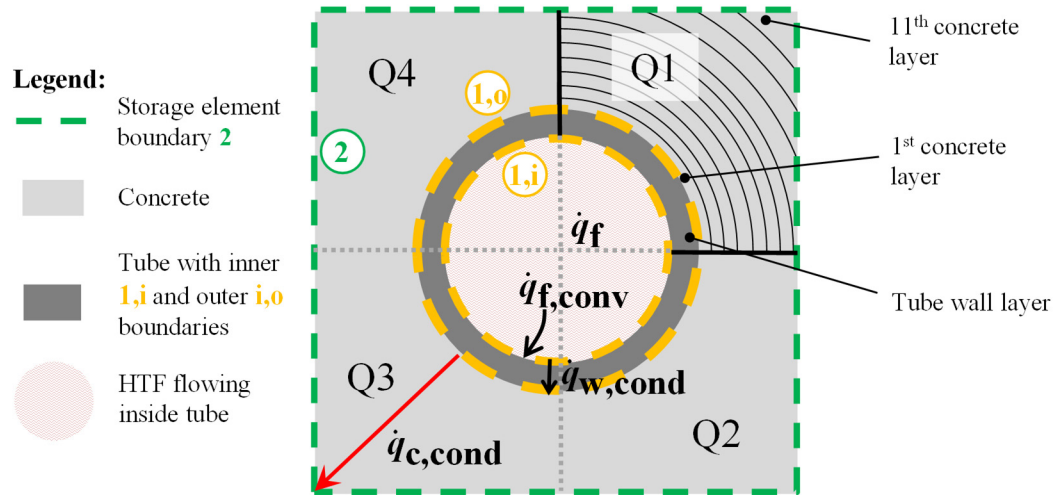


FIGURE 5. Energy balance for a single storage element without insulation (cross-sectional view). A single storage element (SSE) consists of a tube with a square concrete section around. The SSE is divided into 4 quarters (Q1 to Q4) with each quarter composed of 11 concrete layers. (© SIJ)

The kettle-type boiler model is an adaptation of an existing boiler model from the standard Modelica[®] library [10]. The boiler consists of a shell and a tube bundle. To calculate the total energy transfer from the oil-carrying tubes to the water volume inside the shell, the heat transfer coefficient for nucleate boiling was implemented using the equations from Gorenflo (2013) and Fritz (1963) [11,12]. The equations are based on empirical correlations and are dependent on the heat flux as well as the vapour pressure. A two-phase evaporator model calculates the total steam generation using the evaporation enthalpy of water [13]. The evaporator is connected to a non-return valve, which only opens when the steam pressure from the boiler exceeds the pressure of the consumer's steam pipeline.

VALIDATION RESULTS FROM THE COMMISSIONING PHASE

In a commissioning test on a sunny, cloudless day with calm wind conditions, the operation mode of the plant was set to PTC-and-boiler-only (i.e. without C-TES). The purpose of the test was to observe the behaviour of both the PTC and the boiler while maintaining a near-constant oil mass flow. The simulation model was validated with measurement values from this test. To validate the simulation model step by step, first the PTC was isolated as a component. The initial conditions of the real system, the weather and mirror reflectivity data as well as the thermal oil temperature measurement values at the collector inlet (T2) were used as input. The temperature at the collector outlet (T1) was simulated and the corresponding oil temperature difference between the outlet and inlet, i.e. $T1-T2$ or $\Delta T_{oil,PTC}$, was computed. The results are shown in Fig. 6 (a–d) and described below.

As seen in Fig. 6 (a), the DNI drops steadily from 817 to 719 W/m² between 13:50 and 15:47 (Eastern European Summer Time) while the mass flow rate fluctuates between 1.13 and 1.3 kg/s (see Fig. 6 (b)). The drop in DNI along with the near-constant mass flow rate of the thermal oil leads to a decrease of $\Delta T_{oil,PTC}$ from around 50K to 43K as shown in Fig. 6 (c). The dashed line in Fig. 6 (c) represents the simulated $\Delta T_{oil,PTC}$ which shows good agreement with the measurement values between 14:26 until 15:34. When comparing the deviation of the simulated to measured temperature differences, the root mean square (rms) deviation is only 3.86% (equivalent to about 1.9K). The maximum deviation is 11.2% (equivalent to 5.82K) at 14:11, which is rather high. The simulation model will be further refined to improve on the simulation accuracy.

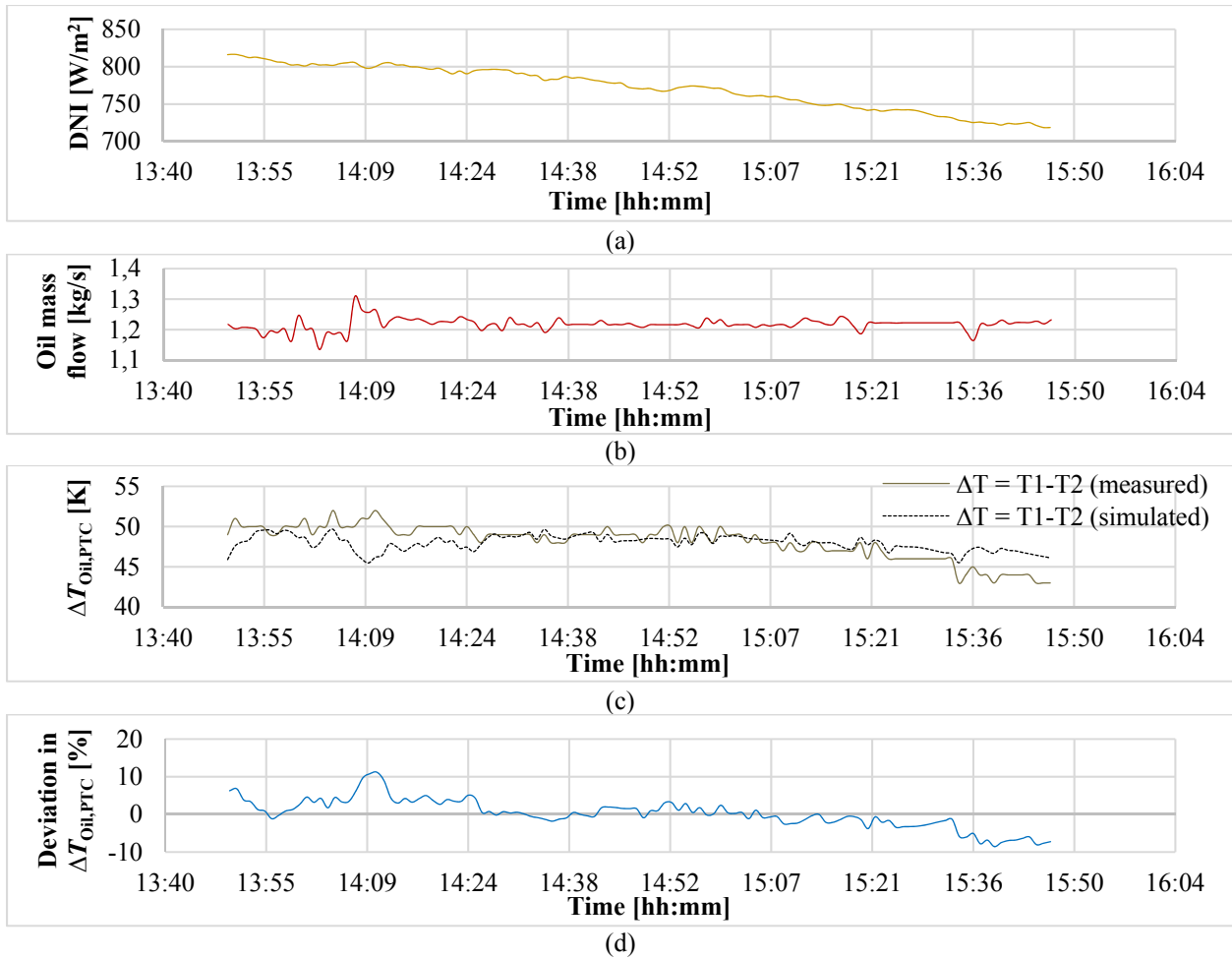


FIGURE 6. (a) DNI for 13:50 – 15:47 local time on a sunny day, (b) Oil mass flow, (c) Comparison of measured vs simulated oil temperature difference $\Delta T_{Oil,PTC} = T1-T2$ between PTC outlet and inlet, (d) Deviation between measurement and simulated oil temperature difference $\Delta T_{Oil,PTC} = T1-T2$ between PTC outlet and inlet. [14]

Following the PTC validation, the boiler was then validated using the complete simulation model in PTC-and-boiler operation only mode. In this simulation, the complete oil cycle is being considered which includes the heat transfer from the oil to the boiler for steam production. Unlike in the isolated PTC-only case, the oil inlet temperature (T2) is no longer a simulation input but is being computed and compared to the T2 measurement values. Fig. 7 shows the simulated oil temperature difference between the PTC outlet to the PTC inlet compared to the measured values. The result of the simulation is a deviation $< 4.25\%$ (rms) between measured to simulated values of $\Delta T_{Oil,PTC}$.

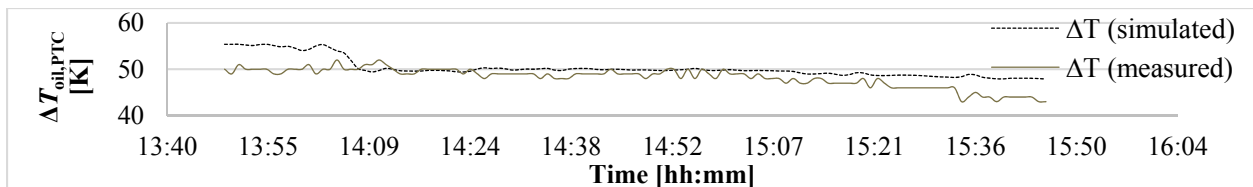


FIGURE 7. Comparison of measured vs simulated oil temperature difference $\Delta T_{Oil,PTC} = T1-T2$ between the PTC outlet and PTC inlet [14]

The storage model was validated as a stand-alone component outside the above described measurement campaign with data from CADE. The deviation between measurement and simulated values is $< 5\%$ compared to the design

point. A case was simulated for 75 kW thermal charging power. The total energy stored after 8 hours is 593.8 kWh which deviates only by 2.7% from the design values for the same conditions.

ACKNOWLEDGMENTS

The project partners and authors would like to express their sincere gratitude for the public funds that were received to-date for carrying out the industrial research project titled *Evaluation of the Dispatchability of a Parabolic Trough Collector System with Concrete Storage* (EDITOR). The international project EDITOR is funded by the Research Promotion Foundation (RPF) from Cyprus, the Ministry of Economy and Competitiveness (MINECO) from Spain, the Federal Ministry for Economic Affairs and Energy (BMWi) from Germany as well as the Ministry of Innovation, Science and Research of the German State of North Rhine-Westphalia from Germany. SOLAR-ERA.NET, a European network that brings together funding organisations, is supported by the European Commission within the EU Framework Programme for Research and Innovation HORIZON 2020 (Cofund ERA-NET Action, N° 691664 and N° 786483) [15].

REFERENCES

1. Solar Thermal Plants Database, <http://ship-plants.info/solar-thermal-plants-map> (Last opened on 14 February 2018).
2. R. Forristall, "Heat Transfer Analysis and Modelling of a Parabolic Trough Solar Receiver Implemented in Engineering Equation Solver" (NREL Technical Paper, NREL/TP-550-34169, 2003).
3. B. W. Stine and R. W. Harrigan, "Solar Energy Fundamentals and Design", (New York: John Wiley & Sons, 1985).
4. S. Caron and M. Röger, "Modelling, Simulation and Identification of Heat Loss Mechanisms for Parabolic Trough Receivers Installed in Concentrated Solar Power Plants" in *IFAC Conference Proceedings online* (8 (1), Vienna, 2015), pp. 372–377.
5. V. Quaschnig, "Regenerative Energiesysteme: Technologie – Berechnung – Simulation", 8., aktualisierte und erweiterte Auflage (Hanser Verlag München, 2013).
6. R. Vasquez Padilla, "Simplified Methodology for Designing Parabolic Trough Solar Power Plants", Ph.D. thesis, University of South Florida, USA, and Universidad del Norte, Baranquilla, Colombia, 2011.
7. Y. A. Çengel, A. J. Ghajar, "Heat and Mass Transfer – Fundamental & Applications", Fifth Edition in SI Units (New York, NY : Mcgraw Hill Education, 944 pages 2015).
8. MDI Weather Station, <http://www.cspservices.de/products-services/measurement-systems/mdi> (Last opened on 15 August 2018).
9. C. Gowtham, "Development of a ray-tracing tool for computing shadow cast on a parabolic trough collector during the course of the day and year", Assignment, Solar-Institut Jülich of the Aachen University of Applied Sciences, 2017.
10. R. Franke, M. Rode and K. Krueger, "On-line Optimization of Drum Boiler Startup", in *3rd International Modelica Conference* (Linköping, 2003).
11. D. Gorenflo, "Behältersieden (Sieden in freier Konvektion)", in VDI-Wärmeatlas, Eleventh Edition (Springer-Verlag, Berlin Heidelberg, 2013).
12. W. Fritz, "Blasenverdampfung (nucleate boiling) im Sättigungszustand der Flüssigkeit an einfachen Heizflächen", in VDI-Wärmeatlas, First Edition (VDI-Verlag, Düsseldorf, 1963).
13. K. J. Åström and R. D. Bell, "Drum-boiler dynamics", in *Automatica* 36 (2000), pp. 363–378.
14. V. N. Atti, "Simulation of a Parabolic Trough collector System with Concrete Thermal Energy Storage for Steam Generation using Modelica", Master's thesis, Solar-Institut Jülich of the Aachen University of Applied Sciences, 2018.
15. SOLAR-ERA.NET network, <http://www.solar-era.net/> (Last opened on 15 August 2018).